Volume 67, Issue 1, 2023
Journal of Scientific Research
of
The Banaras Hindu University

Study on structural, optical and magnetic properties of CdS and Ni-doped CdS nanoparticles

G. Ramalingaiah[1,2]*, K. Sunil Kumar[1], , G.Venkata Ramana[2], A. Narasimhulu[3], R.P. Vijayalakshmi[1]*

1. Dept.Of Physics, Sri Venkateswara University, Tirupati-517502, India.
2. Dept. OfPhysics, SCNR Govt. Degree College, Proddatur-516360, India.
3. Dept. Of Physics, MRR Govt. Degree College, Udayagiri-524226, India.
*Corresponding Author E-mail: ram.gangireddy@gmail.com, vijayaraguru@gmail.com.

Abstract:

The non-noble metal Ni doped CdS (Ni = 0.0, 2.5, 5 and 7.5 at. %) nanoparticleshave been successfully synthesized by a chemical co-precipitation method and were characterized. XRD, SEM, TEM and EDAX analysis were used to study structure, morphology and compositional analysis.The Photoluminescence (PL)properties have been studied by using a fluorescence spectrometer with Xe lamp at 340 nm excitation wavelength, intense PL emission around 495, 620 and 680 nm has been observed in prepared samples. The band gap of prepared nanoparticles are estimated by DRS spectroscopy. FTIR analysis has been carried out on synthesized nanoparticles to confirm presence of functional groups. The magnetic properties of the samples were carried out using vibrating sample magnetometer.These studies indicated the ferromagnetism in CdS: Ni samples. The results shows that as-synthesized Nanoparticles may be useful in the field solar cells, antireflection coatings and spintronics.

Keywords: Chemical method of CdS: Ni Nanoparticles, XRD, TEM, EDAX, PL and VSM.

1.0 Introduction:

Nano semiconductor devices have attained much interest as theyexhibits the electrical and magnetic materials involving electron charge. In contrast, dilute magnetic semiconductor (DMS) materials are the source of spintronic devices [1-3]. DMS has great attention due to its essential strategic role in fabricatingdata storage devices [4]. In II-VI group semiconductors, CdS is one of the most prominent materials having bandgap energy of 2.42 eV at room temperature withan excitation Bohr radius of 5.8 nm [5-6] and it can possess either hexagonal wurtzite or cubic zinc blend structure. CdS has much interest due to its potential applications like nonlinear optical devices [7], flat panel displays[8], light emitting diodes[9-10], solar cells[11], photocatalysis [12], photovoltaic cells [13], photoconductors [14], X-ray detectors [15] etc.,

CdS is the best host material which is used to prepare transition metal-doped semiconductors. Doping of non-noble transition metals (Fe, Mn, Co, Cr, Ni, etc.,) in semiconductors showa significant role in the magnetic behaviour by influencing the optical and luminescence properties. Here we discussed on CdS doped materials synthesized by chemical method. Devadoss et.al [16] were reported on structural, morphological and optical properties of Sn doped CdS:Zn nanoparticles by chemical co-precipitation method. S K Mishra et.al [17] were reported on structural, optical and photoconductivity of Mn doped CdS nanoparticles by chemical co-precipitation method. R S Ibrahim et.al [18] were reported on structural, optical and magnetic properties of Mn doped CdS nanoparticles by chemical co-precipitation method. B S Rao et.al [19] were reported on optical and photoluminescencepropertiesof Ni doped CdS nanoparticles by chemical co-precipitation method. K Suresh et.al [20] were reported on optical propertiesof Ni doped CdS nanoparticles by chemical co-precipitation method. A Goyal et.al [21] were reported on structural and optical propertiesof Cu doped CdS nanoparticles by chemical co-precipitation method. M Thambidurai et.al [22] were reported on structural, optical and electrical properties of Co doped CdS nanoparticles by chemical co-precipitation method. F Arfat et.al [23] were reported on electrical and optical properties of Ni doped CdS nanoparticles by chemical co-precipitation method. Our research group [24] was also reported on different capped CdS nanoparticles synthesized by the chemical co-precipitation method. A few reports are available on Ni doped CdS nanoparticles by chemical co-precipitation method, but there are no reports on detailed magnetic properties of Ni doped CdS nanoparticles synthesized bychemical co-precipitation method, and the present work aims to improve of magnetization and photoluminescence properties.In the present studyNi doped CdSNanoparticleswere prepared by chemical co-precipitation method. Structural, morphological, optical and magnetic behaviour of CdS: Ni Nanoparticles were studied.

2.0 Experimental

2.1 Materials:

Cadmium acetate dehydrate [$Cd(CH_3COO)_2.2H_2O$, 99%], Nickel acetate tetrahydrate [$Ni(CH_3COO)_2.4H_2O$, 98.5%], Sodium sulfide ($Na_2S.9H_2O$)and Polyethylene glycol (PEG) were of analytical grade and used as received without further purification.

2.2 Experimental procedure:

In the present investigation,CdS:Ni(Ni=0.0, 2.5, 5 and 7.5 at. %) The nanoparticles were prepared by a simple chemical co-precipitation method using polyethylene glycol (PEG) as a capping agent [25].

In a typical synthesis, the desired molar ratio$Cd(CH_3COO)_2\cdot 2H_2O$ + $Ni(CH_3COO)_2\cdot 4H_2O$ andNa_2S each was dissolved in 50 ml of deionized water to give 0.2 M, then the solution was stirred for 30 minutes. Subsequently, at the room temperature the Na_2S solution was added dropwise to the solution. Also an adequate amount of stabilizer (PEG) was added to control the growth of nanoparticles during the reaction under constant stirring for 8 hours to obtain fine precipitate. The products were washed several times with deionized water and then the powder was vacuum dried at 80 °C for 10 h to obtain Ni-doped CdS nanoparticles.The detailed synthesis procedure is shown in **Scheme-1**. The proposed stoichiometric synthesis reactions of CdS and CdS: Ni is:

$Cd\ (CH_3COO)_2\cdot 2H_2O + Na_2S\cdot 9H_2O \rightarrow CdS\downarrow + 2NaOH + 8H_2\uparrow + 4CO_2\uparrow + 5H_2O$

$Cd\ (CH_3COO)_2\cdot 2H_2O + Na_2S\cdot 9H_2O + Ni(CH_3COO)_2\cdot 4H_2O \rightarrow$ CdS: Ni $\downarrow + 2NaOH + 15H_2\uparrow + 8CO_2\uparrow + 5H_2O$

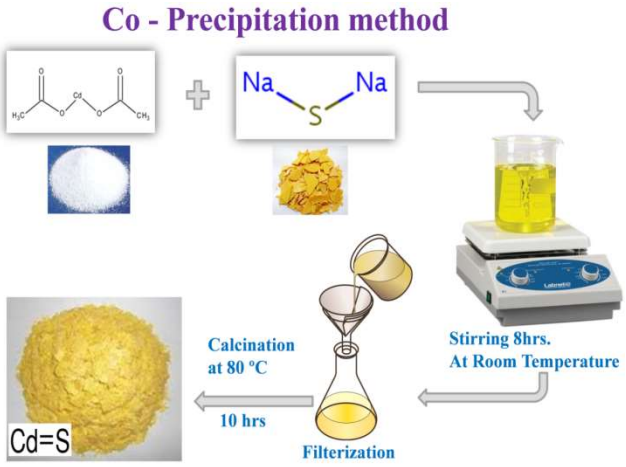

Scheme-1: Schematic representation of the synthesis of pure CdS nanoparticles

2.3 Characterization:

X-ray diffraction(XRD)patterns for the prepared samples were recorded using **RIGAKU; Miniflex-600**XRD with Cu-Kα (λ=1.5406 Å) radiation. Surface morphology and microstructure were observed using scanning electron microscopy (SEM) with EDAX attachment (Model CARL-ZEISS EVO MA 15)and transmissionelectron microscopy (TEM, JEM-2010).The elemental analysis was recorded with Energy Dispersive Analysis of X-rays (EDAX). The functional groupcharacterization of the samples was determined by using FTIR spectra (Model Thermo Nicolet FTIR-200). Optical bandgaps were observed using UV-VIS DRS spectra (Model Carey-5E UV-VIS-NIR Lambda-950). The Photoluminescence spectra was used for determination of emission wavelength of prepared samples (Horiba Jobin-Yvon Fluorolog-3 Spectro fluorometer).VSM was employed to analyze Magnetization Measurements at room temperature (Model VSM-7410).

3.0 Results and discussion:

3.1 Structural analysis:

The XRD patterns are shown in **Fig.1(a)**. It can be observed that all samples displayed an identical XRD spectrum with three diffraction peaks at 2θ values of 26.45° 43.91° and 51.96°of (111), (220) and (311) planes corresponding to the cubic structure with the FCC (JCPDScard No.75-1546). The average nanoparticle size is calculated from the stronger (111) (Fig. 1(b)) peak using the Scherrer's equation, which is in the range of 3.0-4.5 nm(**Table-1**).

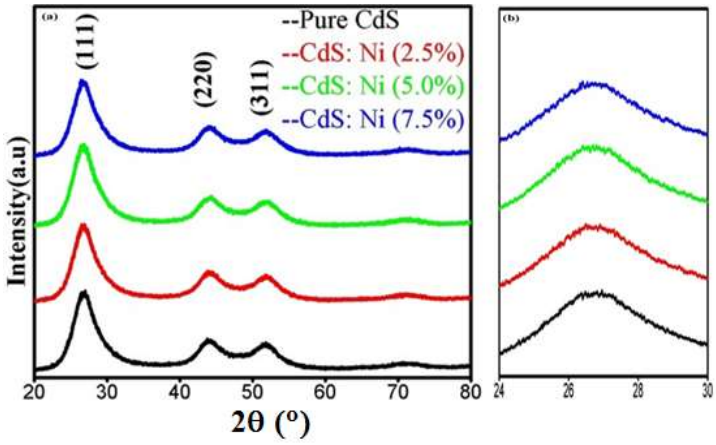

Fig. 1 (a) XRD pattern of CdS and CdS: Ni nanoparticles (b) Enlarged broadening peat 2θ at 26.45°

Table-1: Structural parameters of CdS and CdS: Ni nanoparticles.

sample	2θ (°) (111)	d (Å) (111)	Lattice parameters a =b=c (Å)	Crystal lite size (D) (nm)
Pure CdS	26.45	3.36	5.83	3.0
CdS: Ni (2.5%)	26.50	3.27	5.79	4.0
CdS: Ni (5.0%)	27.16	3.27	5.78	4.4
CdS: Ni (7.5%)	27.20	3.28	5.77	4.5

Further, close examination revealed that all peak positions of CdS: Ni are slightly shifted towards higher 2θ values compared to pristine CdS with increasing Ni dopant concentration. The lattice parameters determined for all samples confirmthe lattice

compression phenomenon in CdS with increasing the Ni dopant concentration(**Table-1**).This phenomenon indicates the successful substitution of smaller size Ni^{2+} (ionic radius: 0.69 Å) ions for higher size Cd^{2+} (ionic radius: 0.97 Å) ionsunder six S^{2-} coordination environment [26-27]. The absence of nickel oxides, nickel sulfides or nickel clusters in the XRD spectra confirms the purity of Ni-doped CdS samples.

.2 Elemental analysis:

The chemical compositions of pure CdS and Ni (2.5 %, 5 % and 7.5 %) doped CdS were characterized by EDAX spectra shown in **Fig.2**. The figure concludes that pure CdS and Ni-doped CdS nanoparticles have to constitute elements without any other elements and agree with XRD analysis. This leads to the effective formation of Ni-doped CdS nanoparticles with appreciable quality and quantity

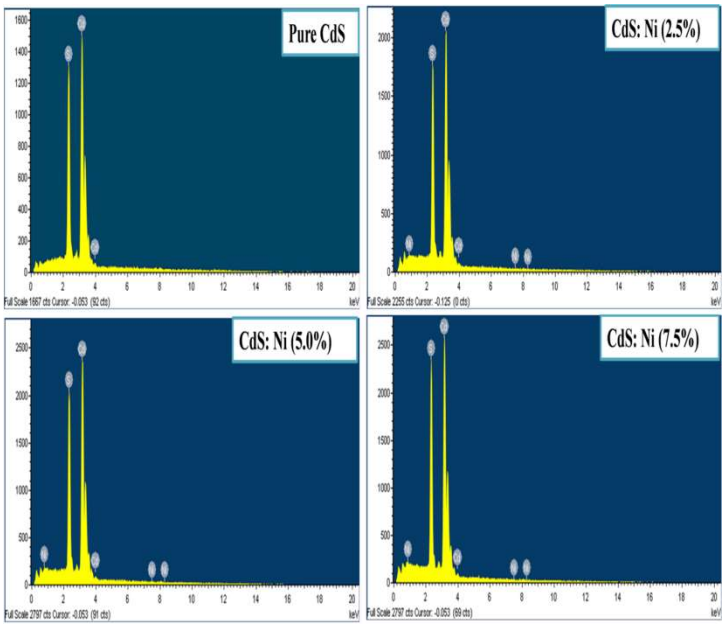

Fig.2 EDAX spectrum of CdS and CdS: Ni

3.3 Morphological studies:

The surface morphology and grain sizes of pure CdS and Ni-doped CdS nanoparticles were characterized by Scanning Electron Microscope (SEM) and Transmission Electron Microscope (TEM) analysis.

Fig. 3 shows the SEM images of pure CdS and Ni (2.5 %, 5 % and 7.5 %) doped CdS nanoparticles. The SEM micrograph indicates that the pure CdS and Ni-doped CdS nanoparticles have spherical shape. It is also noted that 5% Ni-doped CdS nanoparticles are with less agglomeration

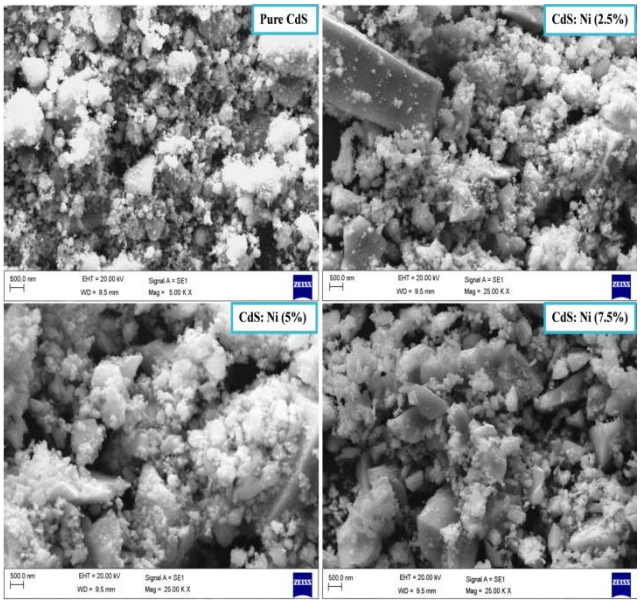

Fig.3SEM images of CdS and CdS: Ni nanoparticles

TEM measurements were also performed to confirm the nanocrystalline structure and morphology of the prepared nanoparticles. Fig. 4(a) shows the interplanar spacing of Ni (5%) doped CdS nanoparticles. The measured interlayer spacing d_{111} = 0.354 nm is consistent with calculated theoretical d_{111} = 0.354 nm [28].TEM images of Ni (5%) doped CdS nanoparticles are shown in **Fig. 4(b&c).** TEM picturesrevealed that the particles were found to be well separated and nearly spherical in shape and the estimated particle size was found to be around 5 nm and this result correlates with X-ray diffraction studies.Fig. 4(d) shows the selected area electron diffraction (SAED) pattern of Ni (5 %) doped CdS nanoparticles the ring pattern indicates the cubic structure [which are well matched with JCPDS card No. 75-1546]. The reflection of (111), (220) and (311) planes can be seen in the SAED pattern of the CdS nanocrystals which agreed well with the XRD pattern.We observed d-spacing values with help of image-J software and is good agreement with XRD values

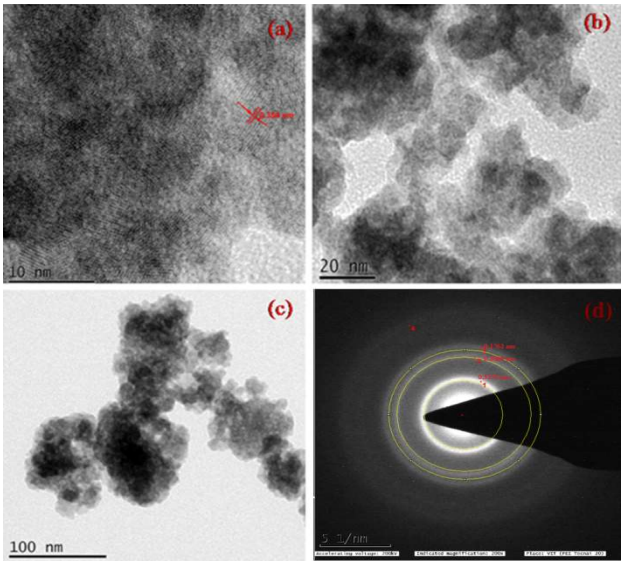

Fig.4 TEM images (a) interplanar spacing, (b) & (C) TEM image and (d) SAED pattern of CdS: Ni (5 %) nanoparticles.

3.3 FTIR Analysis:

FTIR analysis was performed to determine organic contaminants and polymeric components of the prepared nanoparticles. **Fig. 5**shows the FTIR spectra of CdS:Ni nanoparticles were recorded in the range of 4000 to 500 cm^{-1}. All samples showed relatively significant broad absorption peaks around 3447 cm^{-1}, and weaker features around 2360 $cm^{-1}$and 1550-500 cm^{-1}. The peak observed at 624 cm^{-1} is related to the Cd-S stretching mode [29]. The broad absorption peak of 3463 cm^{-1} can be attributed to the O-H vibrational mode, which specifies the amount of water absorbed at the nanoparticle surface. The peaks observed at 2360 cm^{-1} for all samples may be due to the C-H stretching vibration of the alkyl group,due to low annealing temperature the alkyl groups were not eliminated, similar observations were also reported by other researchers [30]. The strong stretching vibration peak observed at 1116 cm^{-1} may be due to the presence of C-O bonds and N-H bending vibrations. These bending vibrations were found to change from moderate to severe intensity, this bond ranged from 1634 to 1540 cm^{-1} [31]. The weak interaction peak at 2852 cm^{-1} is related to symmetric C-H stretching mode in the presence of PEG.

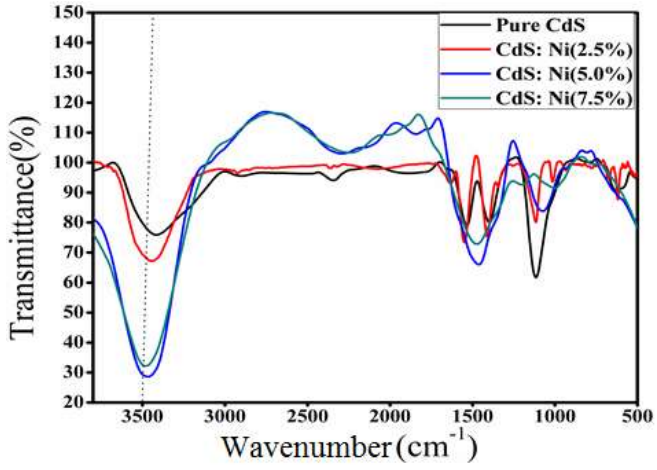

Fig.5: FTIR spectra of CdS and CdS: Ni nanoparticles

3.4 Optical studies:

UV- Vis. Diffuse reflectance spectra of CdS: Ni nanoparticles were shown in **Fig. 6** in the range of 350 to 800 nm.The inset figure shows absorption spectra of pure CdS nanoparticles.The spectrum consists of reflectance edges at the wavelengths of 482.15 nm, 489 nm, 495.9 nm and 500.8 nm,with corresponding energies as 2.57 eV, 2.54 eV, 2.50 eV and 2.48 eV.

The bandgap energy of the Ni-doped CdS nanoparticles was calculated from the diffuse reflectance spectra [32]

$Eg = h\nu = \frac{hc}{\lambda} = \frac{1240}{\lambda} eV$

Where h = Plank constant, C= velocity of light, λ = Cutoff Wavelength

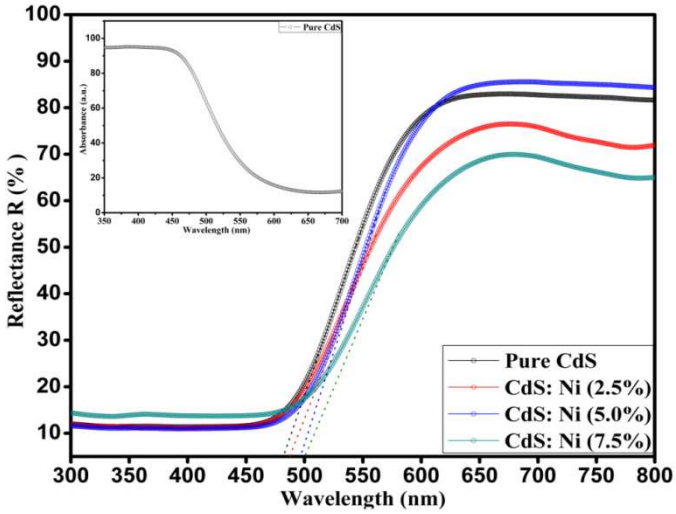

Fig.6: UV-Vis. DRS reflectance spectra of CdS and CdS: Ni nanoparticles.(Insetshows absorbance spectra of CdS nanoparticles.)

The determined bandgap values are tabulated in **Table-2**. The higher bandgap of pure and Ni-doped CdS nanoparticles compared to the bulk CdS (2.42 eV) can be attributed to the quantum confinement due to the smaller size of the particles. As the component atoms are heavier, the bandgap of semiconductors in the group II–VI gets smaller. The quantum size effect causes the bandgap to be larger in the case of nanoparticles with diameters of 2–10 nm compared to the bulk semiconductor.In our samples from XRD studies the particle size is increasing with Ni concentration so the decrease of bandgap with an increasingof the Ni dopant concentrationof CdSmaybe due to the increased particle size [33].

Table-2: Bandgap values of Optical reflectance spectra of pure CdS and CdS: Ni nanoparticles.

Sample	Wavelength (nm)	Bandgap (eV)
Pure CdS	482.2	2.57
CdS: Ni (2.5%)	489.0	2.54
CdS: Ni (5.0%)	495.9	2.50
CdS: Ni (7.5%)	500.8	2.48

3.5 Photoluminescence studies:

Photoluminescence spectroscopy is a very efficient technique to characterize and evaluate the surface quality and energy states between the conduction and valence band.**Fig.7**shows the photoluminescence spectraof CdS: Ni (Ni = 0.0, 2.5, 5 and 7.5 at. %)nanoparticles under the excitation wavelength of 340 nm [34]. All samples exhibited three emission peaks at 495, 622 and 680 nm.

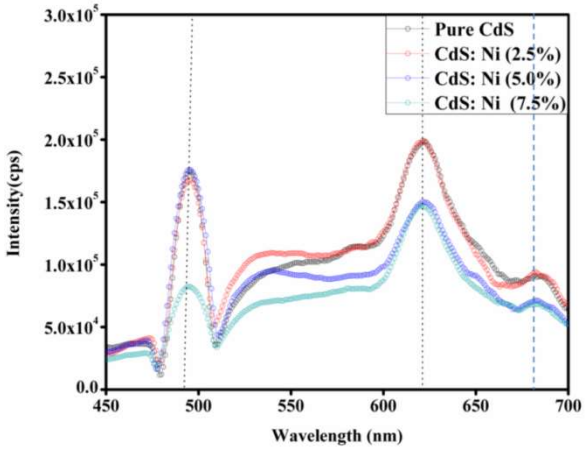

Fig.7: Room temperature Photoluminescence spectra of CdS and CdS: Ni nanoparticles.

The emission peak at 495 nm can be attributed to band edge emission with the radiative recombination of the electron and holes in the valence and the conduction band of CdS. The peak noticed at 527 nm is attributed to the surface trap effect, which contains the recombination of electrons captured in the vacancy of sulfur with a hole in the valence band of CdS and CdS: Ni nanoparticles. The red emission-related peak is observed at around 680 nm, associated with the surface defects of cadmium and sulfur[35-36].The observed peak positions and their intensities are listed in Table-3 with Ni-doping concentration. The spectra show that the peak intensity gradually increases with Ni concentration in the CdS host and attains maximum intensity at 5% Ni dopant.

Table-3: Photoluminescence emission values of CdS and CdS: Ni nanoparticles.

Sample	Emission peak-1 (nm)	Emission peak-2 (nm)
Pure CdS	494	620
CdS: Ni (2.5%)	495	621
CdS: Ni (5.0%)	495	622
CdS: Ni (7.5%)	496	622

3.6 Magnetic studies:

The CdS and Ni-doped CdS nanoparticles magnetic propertieswere characterized by Vibrating Sample Magnetometer with a magnetic field of -15 kG to +15 kGat room temperature. **Fig.8 (a-d)**indicates M-H curves; it represents pure CdS nanoparticles exhibitinga negative hysteresis loop due to diamagnetism. Ni-doped CdS nanoparticles exhibit ferromagnetism at all dopant concentrations (2.5 % Ni, 5 % Ni and 7.5 % of Ni). The ferromagnetism may be due to the alignment of magnetic dipoles on the surface of the nanomaterials.The Ruderman-Kittel-Kasuya-Yosida (RKKY) theory states that the observed room temperature ferromagnetism results from the interaction of locally spin polarised electrons (those doped with ions) and conducting electrons, which are the primary cause of ferromagnetism. The presence of impurities or defects in the hybrid compound affects the magnetism of the free carriers, while the variation in the number of oxygen [37]. These dipoles interact with the nearest alignment in the same direction , which causes ferromagnetism[26-27, 6]. Deka et al. [29] were reportedthetransition metal doped CdS nanocrystals have influenced magnetic properties due to exchange interactions.

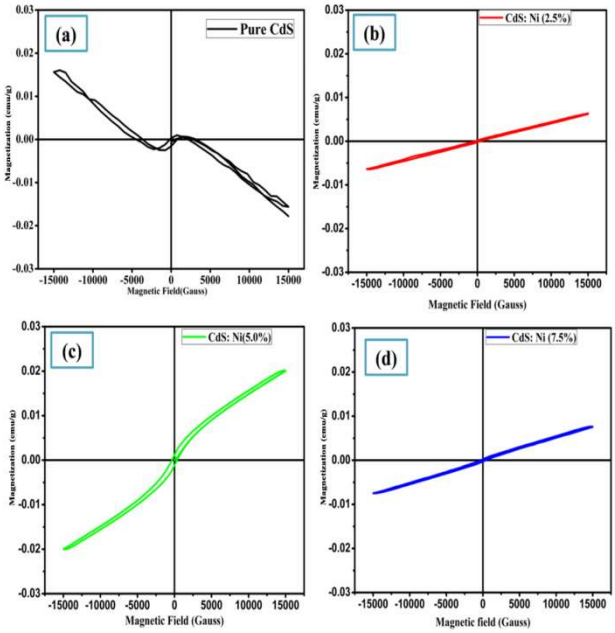

Fig.8(a-d): Vibrating sample magnetometer analysis curves of CdS and CdS:Ni nanoparticles.

The values of coercivity (H_C), retentivity (M_R) and saturation magnetization (M_S) calculated from the M-H curve are shown in Table-4. The value of Hc is increased from 330 to 364 G with an increase of Ni doping concentration from 2.5 to 5% in CdS Nanoparticles and in 7.% of Ni doping Hc is decreased to 349 G . The retentivity and saturation magnetiszation increase with increasing Ni dopantconcentration in CdS Nanoparticles up to 5% and then decreases with further increase of Ni dopant concentration [11].

Table 4: Vibrating sample magnetometer analysis of CdS and CdS: Ni nanoparticles.

Sample	H_C (Oe)	M_R (emu/g)	M_S(emu/g)
Pure CdS	---	---	---
CdS: Ni (2.5%)	330	25.14×10^{-4}	865.9×10^{-4}
CdS: Ni (5.0%)	364	148×10^{-4}	2538×10^{-4}
CdS: Ni (7.5%)	349	29.70×10^{-4}	931.2×10^{-4}

4.0 Conclusions:

In summary, we have successfully prepared CdS (Ni = 0.0, 2.5, 5 and 7.5%) nanoparticles by chemical co-precipitation method.The structure of Pure and CdS: Ni Nanoparticles have cubic zinc blend structure with crystallite sizes around 5 nm from XRD and TEM data. Particles with spherical morphology and homogeneous surface is noticed in the SEM and TEM images. The elemental analysis proved that the corresponding samples are with Cd, S, and Ni. The FTIR spectra confirmed the presence of all functional groups inprepared samples. From DRS studies,we observed that CdS: Ni nanoparticles band gap values were found to be red shifted by 0.09 eV from the pure CdS.The synthesized pure and CdS: Ni nanoparticles have an emission intensity between 495, 620 and 680 nm. From VSM Studies, it is observed that CdS: Ni (5%) nanoparticles possess high ferromagnetism and the value of the magnetic saturation has been found to be 0.0258emu/g. There is wide range of applications for CdS: Ni nanoparticles like solar cells, antireflection coating and spintronics which are of considerable interest.

References:

[1]. Zutic I, Fabian J, Sarma SD,Reviews of modern physics,76(2004)323.

[2]. Ohno H, Munekata H, Penney YT, Von Molnar S, Chang LL, Physical Review Letters, 68(1992)2664.

[3]. Monsma DJ, Vlutters R, Lodder JC, Science, 281(1998)407-9.

[4]. Pan A, Liu D, Liu R, Wang F, Zhu X, Zou B, Small, 1(2005)980-3.

[5]. Geng J, Jia XD, Zhu JJ, Cryst.Eng.Comm, 13(2011)193-8.

[6]. Morales-Acevedo A, Solar energy materials and solar cells, 90(2006)2213-20.

[7]. Lai CH, Huang KW, Cheng JH, Lee CY, Hwang BJ, Chen LJ, Journal of Materials Chemistry,20(2010)6638-45.

[8]. Lin YF, Song J, Ding Y, Lu SY, Wang ZL, Advanced Materials, 20(2008)3127-30.

[9]. Gopal A, Hoshino K, Kim S, Zhang X, Nanotechnology, 20(2009)235201.

[10]. Kar S, Chaudhuri S, Synthesis and Reactivity in Inorganic, Metal-Organic and Nano-Metal Chemistry, 36(2006)289-312.

[11]. Romeo N, Bosio AA, Romeo A, Solar Energy Materials and Solar Cells, 94(2010)2-7.

[12]. Huynh WU, Dittmer JJ, Alivisatos AP, science, 295(2002)2425-7.

[13]. Uda H, Sonomura H, Ikegami S, Measurement Science and Technology, 8(1997)86.

[14]. Lee W, Min SK, Dhas V, Ogale SB, Han SH, Electrochemistry Communications, 11(2009)103-6.

[15]. Seibert MM, Ekeberg T, Maia FR, Svenda M, Andreasson J, Jonsson O, Odic D, Iwan B, Rocker A, Westphal D, Hantke M, Nature, 470(2011)78-81.

[16]. Devadoss I, Sakthivel P, Pauline Sheeba S, Indian Journal of Physics, 95(2021)741-7.

[17]. Mishra SK, Srivastava RK, Prakash SG, Yadav RS, Panday AC, Journal of alloys and compounds, 513 (2012) 118-24.

[18]. Ibrahim RS, Azab AA, Mansour AM, Journal of Materials Science: Materials in Electronics, 32(2021)19980-90.

[19]. Rao BS, Reddy VR, Kumar BR, Rao TS, International Journal of Nanoscience, 11(2012)1240006.

[20]. Kumar S, Sharma JK, Material Science Research India, 14(2017)5-8.

[21]. Goyal A, Sharma V, Sharma A, Agarwal R, Sharma KB, Kothari SL, Journal of Nano-and Electronic Physics, 3(2011)254.

[22]. Thambidurai M, Muthukumarasamy N, Velauthapillai D, Agilan S, Balasundaraprabhu R, Journal of electronic materials, 41(2012)665-72.

[23]. Firdous A, Singh D, Ahmad MM, Applied Nanoscience, 3(2013)13-8.

[24]. Ramalingaiah G, Kumar KS, Ramanadha M, Sudharani A, Vijayalakshmi RP,Journal of Eng. Trends and Tech., 49(2017) 5-10.

[25]. Luo M, Liu Y, Hu J, Liu H, Li J, ACS Applied Materials & Interfaces, 4(2012) 1813-21.

[26]. Singh V, Rathaiah M, Venkatramu V, Haase M, Kim SH, Spectrochimica Acta Part A: Molecular and Biomolecular Spectroscopy, 122 (2014) 704-10.

[27]. Smith BC, CRC press,(2011).

[28]. Zu D, Song H, Wang Y, Chao Z, Li Z, Wang G, Shen Y, Li C, Ma J, Applied Catalysis B: Environmental, 277 (2020) 119140.

[29]. Deka K, Kalita MP, Journal of Alloys and Compounds, 757 (2018) 209-20.

[30]. Tiwary KP, Ali F, Mishra RK, Kumar S, Sharma K, Digest Journal of Nanomaterials and Biostructures, 14(2019)305-13.

[31]. Sankar M, Jothibas M, Muthuvel A, Rajeshwari A, Jeyakumar SJ, Surfaces and Interfaces, 21 (2020) 100775.

[32]. Bhambhani P, Alvi PA, Journal of Optoelectronics Engineering, 4 (2016) 11-6.

[33]. Zhang Z, Ren Y, Han L, Xie G, Zhong B, Physica E: Low-dimensional Systems and Nanostructures, 92 (2017) 30-5.

[34]. Muthusamy M, Muthukumaran S, Optik, 126(2015) 5200-6.

[35]. Rao BS, Reddy VR, Kumar BR, Rao TS, International Journal of Nanoscience, 11(2012)1240006.

[36]. Madhavi J, Prasad V, Reddy KR, Reddy CV, Raghu AV, Journal of Environmental Chemical Engineering, 9(2021)106335.

[37]. Li BB, Xiu XQ, Zhang R, Tao ZK, Chen L, Xie ZL, Zheng YD, Xie Z, Materials science in semiconductor processing, 9(2006)141-5.